Chapter 4

Degenerate (Nonproductive) Reactions with Ruthenium Metathesis Catalysts

The text in this chapter is reproduced in part with permission from:

Stewart, I. C.; Keitz, B. K.; Kuhn, K. M.; Thomas, R. M.; Grubbs, R. H. *J. Am. Chem. Soc.* **2010**, *132*, 8534.

Thomas, R. M.; Keitz, B. K.; Champagne, T.; Grubbs, R. H. *J. Am. Chem. Soc.* **2011**, *133*, 7490.

Abstract

The study of degenerate (nonproductive) metathesis events during ring-closing metathesis (RCM) is discussed. Catalyst structure, specifically with regard to the N-heterocyclic carbene (NHC) ligand, was found to have a significant effect on degenerate versus productive selectivity. For example, catalysts with N-aryl/N-aryl NHC ligands displayed high selectivity for productive metathesis while those with N-aryl/N-alkyl NHC ligands exhibited selectivity for degenerate metathesis. Finally, the relationship between degenerate metathesis and selectivity for kinetic metathesis products is also discussed, along with the application of degenerate-selective catalysts towards the ethenolysis of methyl oletate.

Introduction

Degenerate or nonproductive events are common during both cross metathesis (CM) and ring-closing metathesis (RCM). These events are defined as catalytic turnovers that produce an equivalent of the starting material, but are distinct from simply undergoing the reverse process in an equilibrium reaction. As such, degenerate reactions can only be visualized through isotopic labeling (cross-over) experiments (Figure 4.1). Indeed, with the aid of multiple isotopologues of propylene (e.g., *Z*-d_1,d_2-propene and d_3-propene), the effect of degenerate metathesis during cross-metathesis has been studied extensively for early hetero- and homogeneous molybdenum (Mo) and tungsten (W) catalysts.[1] In these studies, the rate of degenerate metathesis was found to exceed that of productive metathesis by approximately an order of magnitude. Furthermore, evidence was provided for the

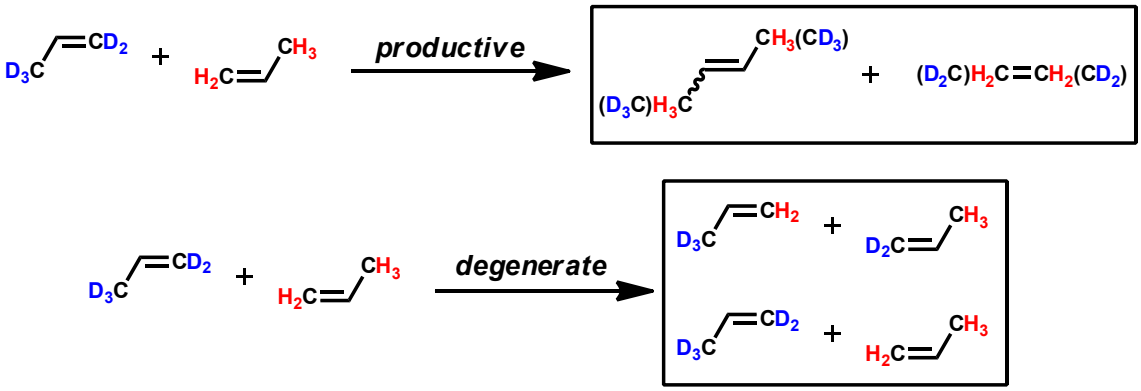

Figure 4.1. (top) Productive metathesis and (bottom) degenerate/nonproductive metathesis (bottom) of propylene

presence of a chain-carrying metal alkylidene intermediate (M=CHR) as opposed to a metal methylidene ($M=CH_2$). While these reports were the first to explore the role of degenerate metathesis, similar studies using modern ruthenium-based olefin metathesis catalysts and synthetically relevant reactions have not been undertaken.

Understanding such degenerate reactivity can provide insight into a number of important catalyst attributes relevant to metathesis reactions. First, catalytic activity, specifically turnover frequency (TOF), is significantly affected by degenerate versus productive selectivity. For instance, a degenerate-selective catalyst (**A**) may perform 10 degenerate turnovers (D-TON) per second and 1 productive turnover (P-TON) per second giving the catalyst a TOF of 1 $[product]\cdot[catalyst]^{-1}\cdot s^{-1}$. In contrast, a productive-selective catalyst (**B**) may have a P-TON of 10 and a D-TON of 1 per second, giving it a TOF of 10 $[product]\cdot[catalyst]^{-1}\cdot s^{-1}$. Clearly, all else being equal, catalyst **B** would be considered superior. A second rationale for studying degenerate metathesis concerns catalyst stability, which can be quantified by the total number of turnovers (TON). Under ideal conditions, degenerate reactions do not cause a net change in the concentration of catalyst. However, under realistic conditions,

they provide additional opportunities for catalyst decomposition. For example, catalyst decomposition can occur directly from ruthenacycle intermediates,[2] so the more time a catalyst exists as this intermediate, the more likely it is to decompose. Furthemore, the species responsible for degenerate metathesis (e.g., $M=CH_2$) are often more prone to decomposition. These examples clearly demonstrate that degenerate metathesis has a significant effect on both catalyst activity and stability. In addition, the Hoveyda and Schrock groups have reported that degenerate processes are essential to achieving high enantioselectivity in asymmetric ring-closing reactions for Mo/W systems.[3] Although less relevant to Ru catalysts, their work further illustrates the importance of studying degenerate metathesis.

Here, we present the first studies of degenerate metathesis in ruthenium-based olefin metathesis catalysts and demonstrate that a catalyst's structure determines its selectivity for either productive or degenerate metathesis. We also show that for some reactions, such as ethenolysis, selectivity for degenerate metathesis is actually advantageous, and that this observation can be used as a foundation from which to develop new industrially relevant catalysts.

Results and Discussion

We chose to initiate our studies on degenerate metathesis by examining the RCM of a deuterium labeled variant of diethyl diallylmalonate (**4.5-d_2**), one of the benchmark substrates for evaluating olefin metathesis catalysts.[4] Compound **4.5-d_2** was prepared by straightforward organic synthesis (Figure 4.2) starting from propargyl alcohol (**4.1**) and deuterium oxide (D_2O). The RCM of **4.5-d_2** entails one productive metathesis pathway and two potential degenerate pathways (Figure

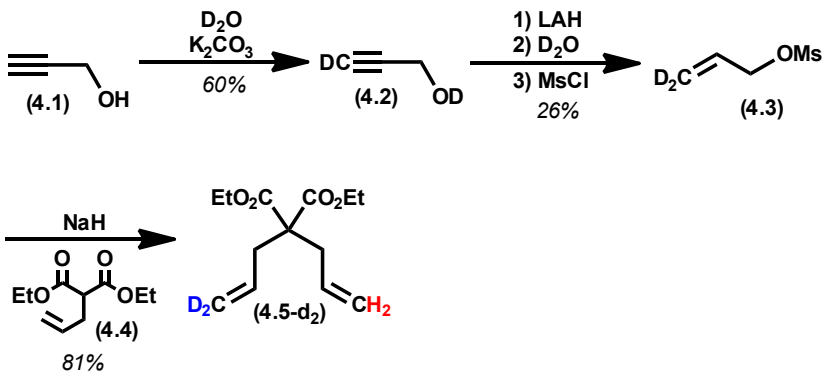

Figure 4.2. Preparation of labeled RCM substrate **4.5-d$_2$**. Ms = methane sulfonyl, LAH = lithium aluminum hydride

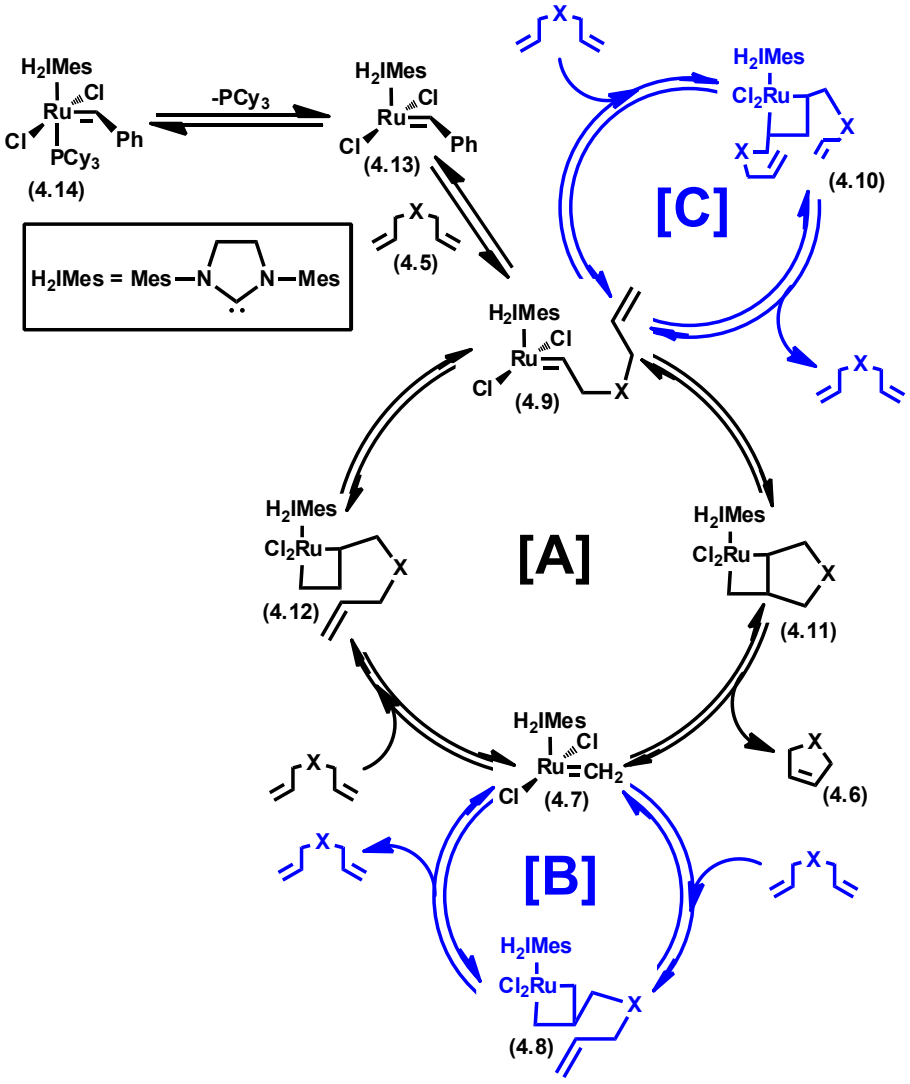

Figure 4.3. (**A**) Productive catalytic cycle for RCM of **4.5** to **4.6** and degenerate cycles starting from (**B**) methylidene (Ru=CH$_2$) and (**C**) alkylidene (R=CHR). Mes = 2,4,6-trimethylphenyl

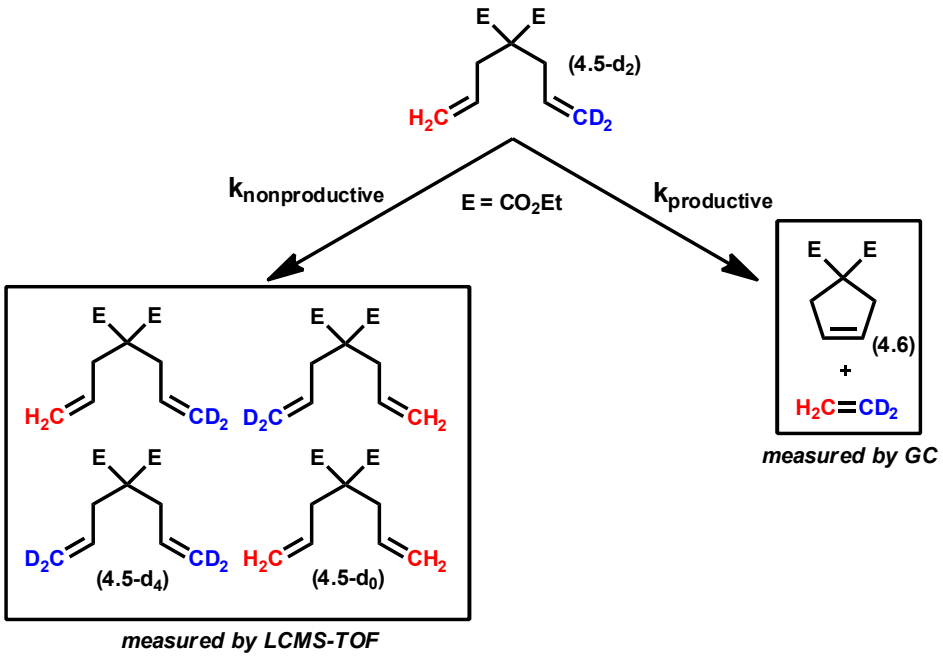

Figure 4.4. Products generated from the degenerate and productive metathesis of **4.5-d$_2$**

4.3). The first degenerative pathway begins with a Ru methylidene (**4.7**) that reacts with an olefin to form a β-substituted ruthenacycle (**4.8**). Subsequent breakdown of this ruthenacycle regenerates the starting material but exchanges the methylene termini. An alternative degenerate pathway begins with a Ru alkylidene (**4.9**) and ends with the retrocycloaddition of an α,α-disubstituted ruthenacycles (**4.10**). Overall, through the combination of productive and degenerative metathesis, a mixture of compounds **4.6**, **4.5-d$_4$**, and **4.5-d$_0$** is generated from the RCM of **4.5-d$_2$** (Figure 4.4).[5]

In order to investigate the dependence of the relative amounts of **4.5-d$_4$**, **4.5-d$_0$** (from degenerate metathesis), and **4.6** (from productive metathesis) on catalyst structure, **4.5-d$_2$** was subjected to catalysts **4.14**–**4.21**. The conversion to cyclopentene **4.6** was monitored by gas chromatography (GC) while the relative

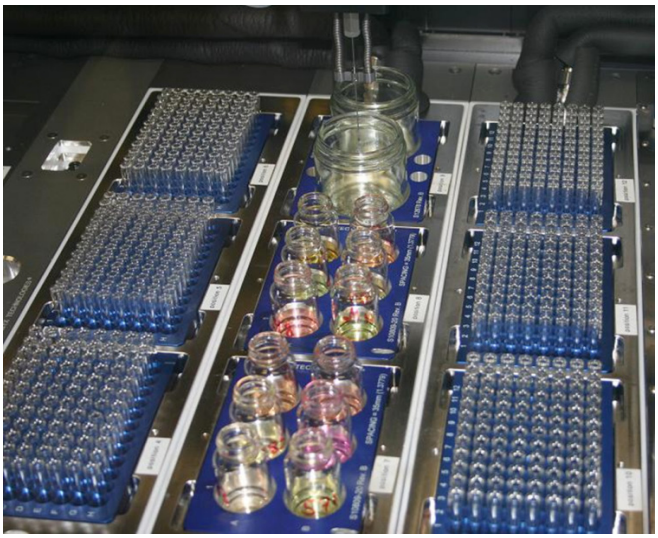

Figure 4.5. Example SYMYX set up of RCM of **4.5-d$_2$** using different catalysts. Reaction solutions are in the middle, flanked by chilled aliquot vials filled with ethyl vinyl ether solutions (in toluene) to quench the catalysts.

amounts of **4.5-d$_4$** and **4.5-d$_0$** were determined by time-of-flight mass spectrometry (TOF-MS). We were aided in the execution of our experiments by the use of a SYMYX robotics core module,[6] which automated the collection of reaction aliquots for multiple catalysts simultaneously and in triplicate (Figure 4.5). Reactions run by hand faithfully reproduced the results from the robot, but were discouraged in lieu of the high degree of reproducibility provided by the robot. The relative amounts of **4.5-d$_4$**, **4.5-d$_0$**, and **4.6** were used to calculate degenerate and productive TON, respectively, and these values were plotted versus one another for each catalyst (Figure 4.6).[7]

As shown in Figure 4.6, the ratio of degenerate to productive TON varied widely as a function of catalyst structure. For example, 'good' catalysts (e.g., **4.14**–**4.17**) displayed remarkable selectivity for productive metathesis over degenerate

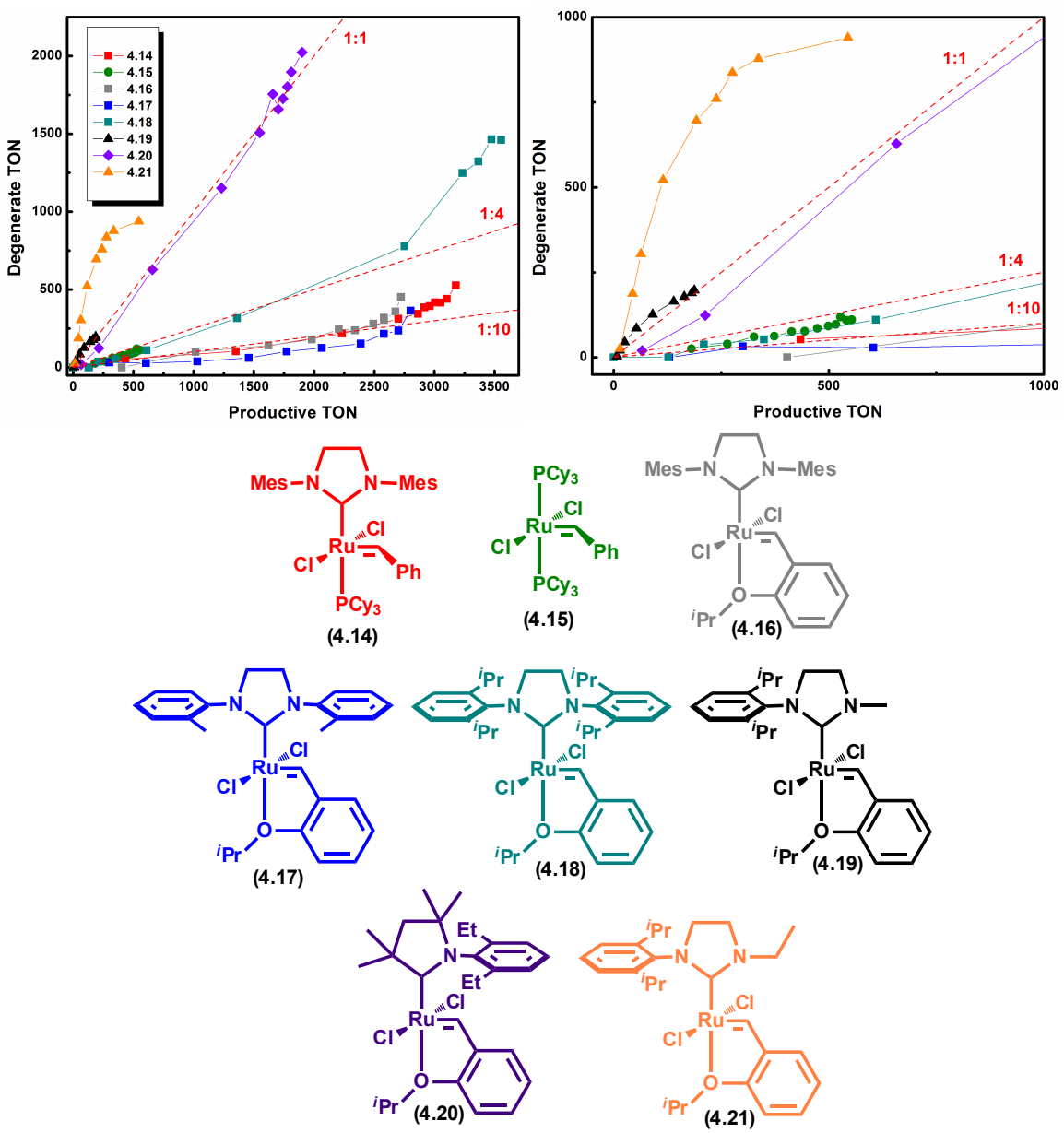

Figure 4.6. (top left) Degenerate TON versus productive TON for the RCM of **4.5-d$_2$** with catalysts **4.14**–**4.21**. (top right) blow up of low TON region. Reaction conditions were 50 °C in toluene (1 mL) with **4.5-d$_2$** (0.1 mmol) and catalyst (**4.15**—1000 ppm, **4.14**, **4.16**, **4.17**, **4.18**—250 ppm, **4.19**—5000 ppm, **4.20**—500 ppm, **4.21**—1000 ppm).

metathesis. This result is consistent with the general evolution of these catalysts, since they would not have been developed and optimized if they were unable to

efficiently perform the RCM of **4.5**. However, small differences were observed among the productive metathesis selective catalysts. Specifically, phosphine containing catalyst **4.15** performed slightly more degenerate TON (falling close to the 1:4 line, Figure 4.6) compared to the NHC-containing catalysts (**4.14**, **4.16**, and **4.17**), which favored productive metathesis (falling on the 1:10 line). However, due to catalyst decomposition, **4.15** did not reach nearly as many total TON, which complicates direct comparisons between the two catalyst types. Nevertheless, the slight preference of catalysts **4.14**, **4.16**, and **4.17** for productive metathesis, along with their higher stability and preference for olefin binding,[8] explains their general superiority in metathesis reactions when compared to **4.15**.

More significant differences were observed between catalysts containing different types and structures of NHCs (**4.16**–**4.21**). For example, switching the aryl group of the NHC from Mes (**4.14**, **4.16**) or ortho-tolyl (**4.17**) to the larger 2,6-diisopropylphenyl (DIPP, **4.18**) resulted in a large increase in selectivity for degenerate metathesis (teal line in Figure 4.6). A more striking change occurred when the NHC was replaced with a cyclic alkyl amino carbene (CAAC, **4.20**). In this case, a 1:1 ratio of degenerative to productive metathesis was achieved. Similar selectivity for degenerate metathesis was measured when catalysts with N-aryl/N-alkyl NHCs (**4.19**, **4.21**) were tested. In addition to being remarkably selective for degenerative metathesis, catalyst **4.21** (orange line) also showed an interesting saturation effect, which we attribute to the achievement of thermodynamic equilibrium between the isotopologues of **4.5**.

Initially, we believed that the increase in degenerate selectivity observed in

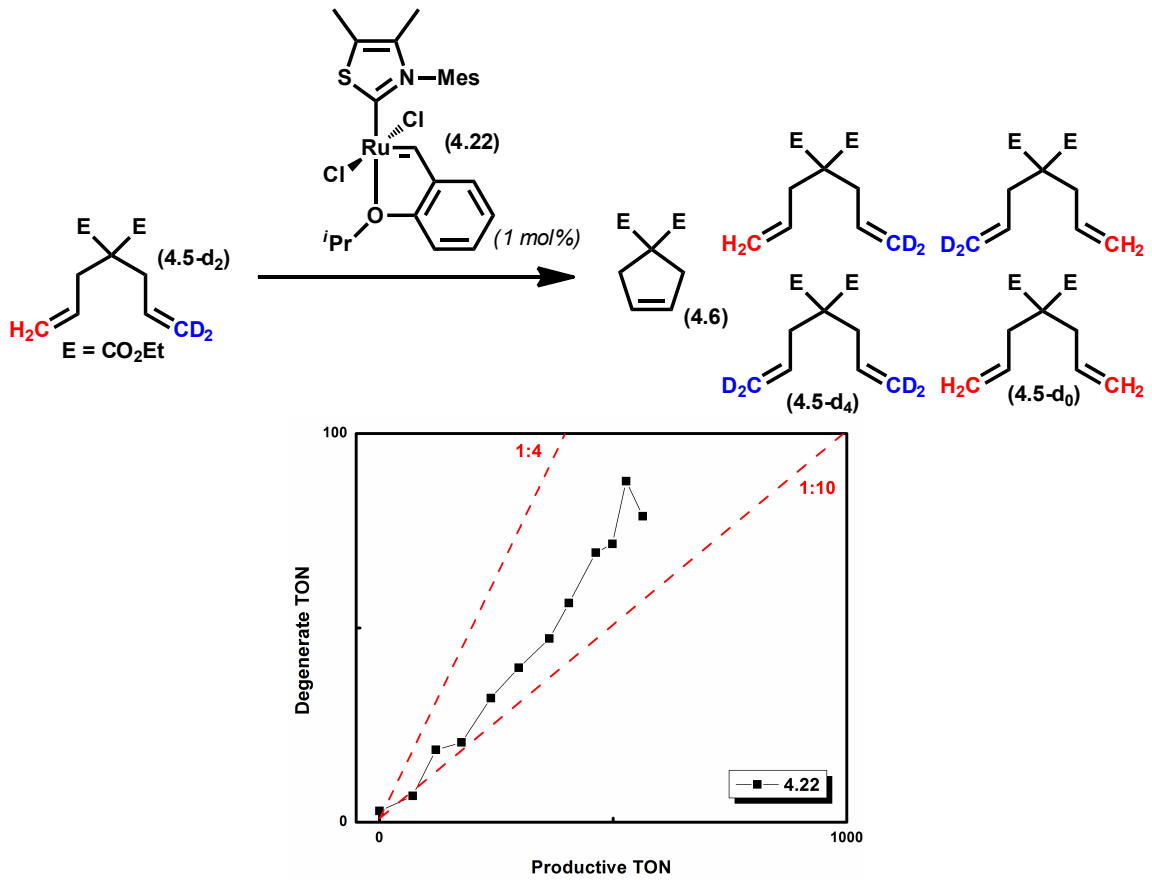

Figure 4.7. RCM of **4.5-d$_2$** with catalyst **4.22** and plot of degenerate versus productive TON

catalysts **4.19**–**4.21** arose from a decrease in the steric environment around the metal center. For instance, catalysts **4.19**–**4.21** contain asymmetric NHCs (or a CAAC) with at least one small N-substituent (methyl in **4.19**, dimethyl in **4.20**, ethyl in **4.21**). In order to examine whether or not this small substituent was responsible for the increase in degenerate selectivity, the thiazolium carbene-based catalyst **4.22** was prepared and subjected to our ring-closing conditions.[9] Unfortunately, catalyst **4.22** was fairly unstable and did not give high total TON (Figure 4.7). However, it was very selective for *productive* metathesis, suggesting that a less congested steric environment does not necessarily result in selectivity for

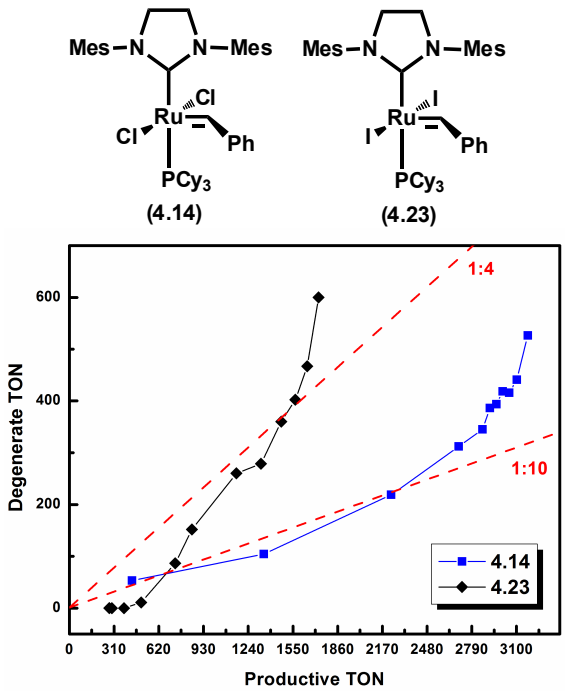

Figure 4.8. RCM of **4.5-d$_2$** and plot of degenerate versus productive TON for catalysts **4.14** and **4.23**

degenerate metathesis. This analysis is obviously complicated by the ability of the NHC to rotate about the C–Ru bond;[7] nevertheless, there is no obvious relationship between the sterics of the NHC and selectivity for degenerate metathesis. Clearly the relationship between catalyst structure and selectivity for degenerate or productive metathesis is more complex, and as such, a more thorough treatment will be presented in Chapter 5. For now we will continue to focus on more empirical results.

Continuing with our goal of evaluating the effect of structural changes on degenerate selectivity, we next focused on the effect of the halide ligands. Iodo-catalyst **4.23** was prepared from **4.14** using sodium iodide (NaI) and subjected to the standard reaction conditions described in Figure 4.6. Figure 4.8 clearly shows that the diiodo catalyst **4.23** is much less selective for productive metathesis.

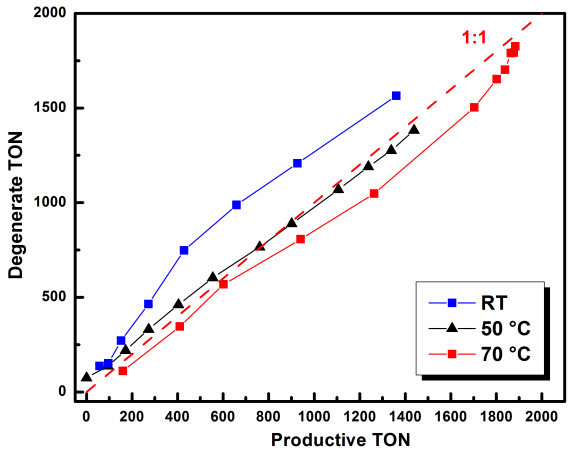

Figure 4.9. RCM of **4.5-d$_2$** with catalyst **4.20** at room temperature (RT), 50 °C, and 70 °C

Catalyst **4.23** is known to initiate faster than **4.14** (k_{obs} of phosphine dissociation) but is less selective for olefin binding over phosphine reassociation.[7] As such, dichloro catalyst **4.14** is generally considered superior to **4.23**. However, catalyst **4.23**'s selectivity for degenerate over productive metathesis may also contribute to its inferiority when compared to **4.14**. Although we do not currently have a mechanistic rationale for the increase in degenerate selectivity, future investigators may wish to study the dynamics of ruthenacycles with halide ligands other than chloride (see Chapter 5).

We next turned to examining the effect of temperature on selectivity for degenerate over productive metathesis. The RCM of **4.5** to **4.6** is both kinetically and thermodynamically favored whereas the degenerate metathesis of **4.5-d$_2$** to **4.5-d$_0$** and **4.5-d$_4$** is essentially thermo-neutral excluding kinetic and thermodynamic isotope effects.[10] Moreover, RCM to **4.6** is functionally irreversible, whereas the isotopologues of **4.5** are in equilibrium. For these reasons and because we cannot observe every degenerate event (e.g., **4.5-d$_2$** to **4.5-d$_2$**), we anticipated that an

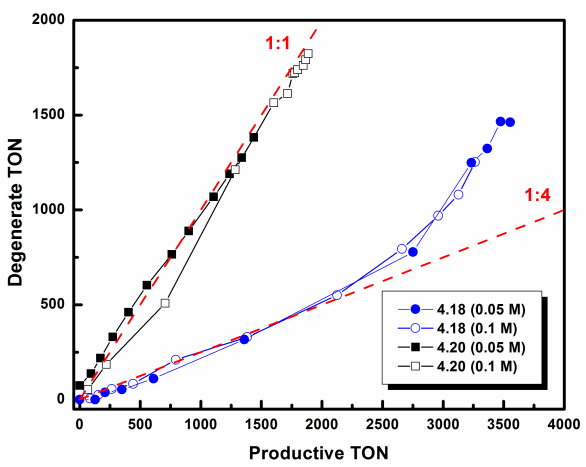

Figure 4.10. RCM of **4.5-d$_2$** with catalysts **4.18** and **4.20** at different substrate concentrations

increase in temperature would result in a small increase in productive metathesis selectivity. To probe this, we performed the RCM of **4.5-d$_2$** with catalyst **4.20**, since this catalyst is relatively selective for degenerate metathesis but is also able to reach very high TON. Indeed, under our standard conditions, catalyst **4.20** displayed a slight increase in productive selectivity as a function of temperature (Figure 4.9). The effect is not dramatic, but does demonstrate that small changes in degenerate selectivity can be affected by changes in temperature.

Following our temperature studies, we next examined the effect of concentration on degenerate metathesis selectivity. As shown in Figure 4.10, no significant change was observed with varying substrate concentration for either catalyst **4.18** or **4.20** in the RCM of **4.5-d$_2$**. This result implies that degenerate metathesis is proceeding through a Ru–methylidene propagating species (e.g., Figure 4.3, B), since an alkylidene propagating species (Figure 4.3, C) would be expected to exhibit some concentration dependence. Both **4.18** and **4.20** are stable as methylidenes, which have also been identified as the propagating species in

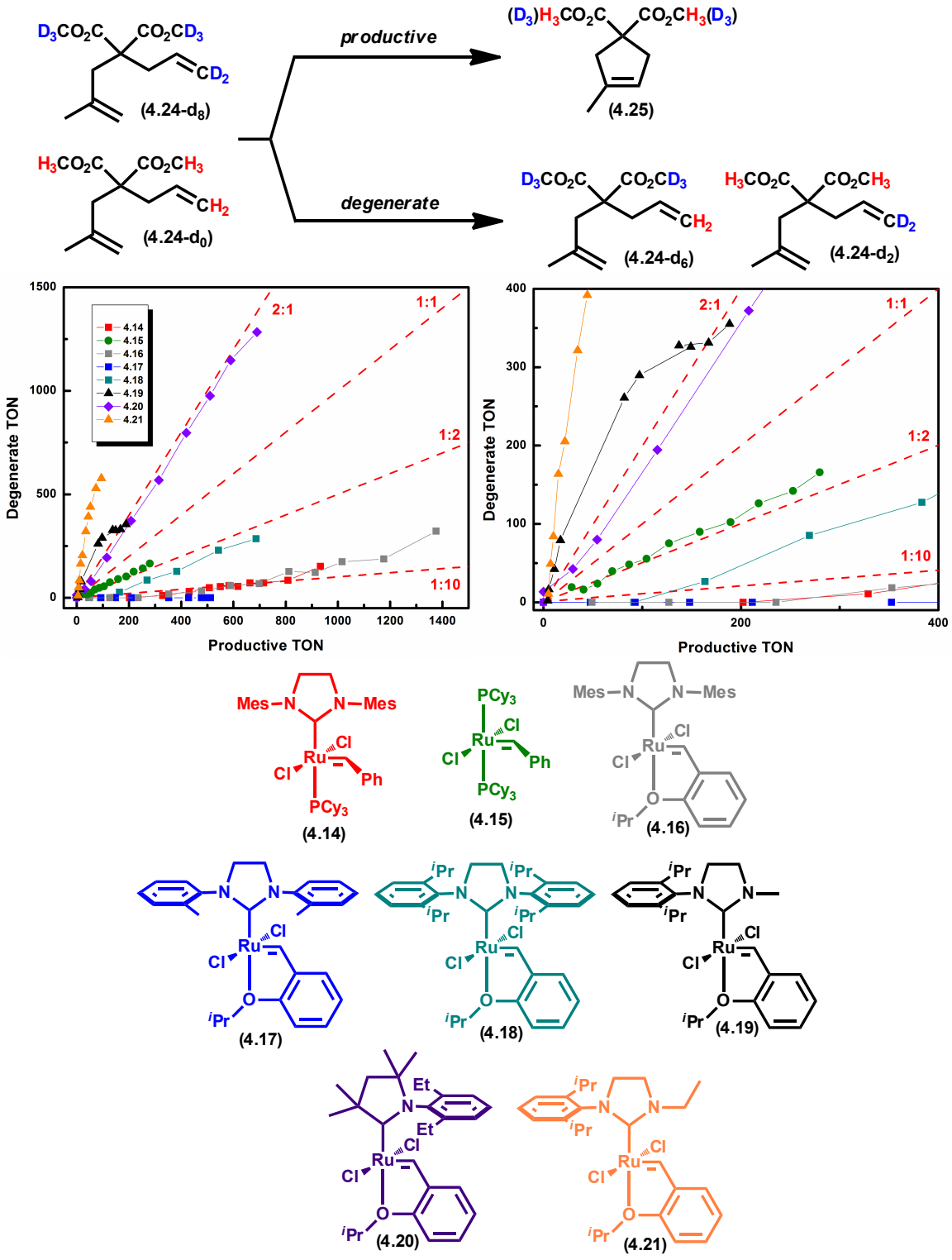

Figure 4.11. (top) RCM of **4.24** to form **4.25**. (bottom) Plot of degenerate TON versus productive TON for the RCM of **4.24-d$_8$** and **4.24-d$_0$**. Reaction conditions were 50 ° in $PhCH_3$ (1 mL) with substrate (0.1 mmol total, **4.24-d$_8$**:**4.24-d$_0$**, 1:1) and catalyst (**4.15**—000 ppm, **4.14**, **4.16**, **4.17**, **4.18**—250 ppm, **4.19**—5000 ppm, **4.20**—500 ppm, **4.21**—1000 ppm)

certain reactions, such as ethenolysis.[11] However, recall that an alkylidene complex was proposed as the active degenerate species in heterogeneous metathesis catalysts. Therefore, despite the above results favoring a methylidene, new assays will need to be developed that are more sensitive over a larger concentration regime in order to precisely determine the species responsible for degenerate metathesis.

In order to evaluate the effect of degenerate metathesis in a more challenging reaction, the RCM of **4.24** was attempted. For this reaction, a mixture of **4.24-d_8** and **4.24-d_0**, which were prepared in an analogous manner to **4.5**, were subjected to catalysts **4.14**–**4.21**. As before, productive metathesis was measured by GC while degenerate metathesis (to **4.24-d_6** and **4.24-d_2**) was monitored by LCMS-TOF (Figure 4.11). In line with previous results for substrate **4.5-d_2**, NHC catalysts **4.14**, **4.16**, and **4.17** performed the fewest degenerate events. In the case of catalyst **4.17**, almost no degenerate reactions were detected. Bulky NHC-bearing catalyst **4.18** and bisphosphine catalyst **4.15** performed around one degenerate reaction for every two productive turnovers. Catalysts **4.19**–**4.21**, on the other hand, perform two or more degenerate reactions for every productive RCM event. Overall, the relative differences in selectivity between catalysts were the same as in the RCM of **4.5**. However, the ratio of degenerate to productive TON was typically larger in the case of **4.24**, which reflects the increased difficulty of this RCM reaction. In other words, there are more opportunities for degenerate metathesis because the RCM of **4.24** is comparatively slow.

Kinetic Modeling

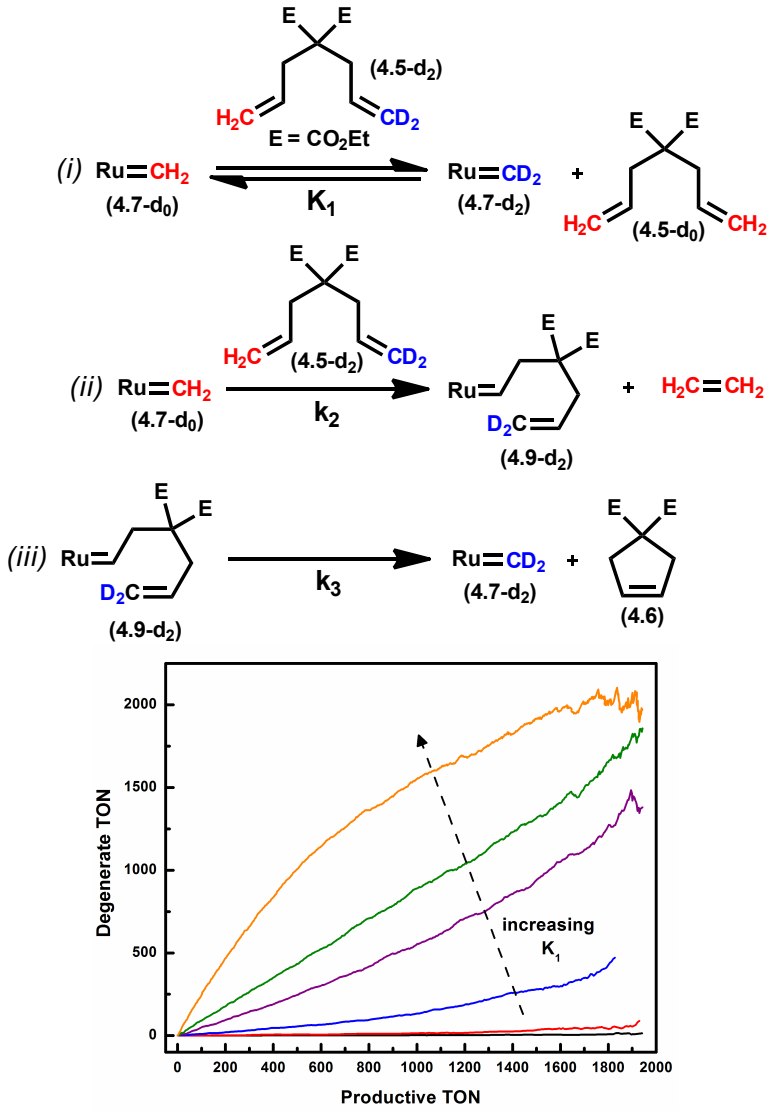

Figure 4.12. Simplified kinetic model for RCM of **4.5-d$_2$**. See experimental section for complete model. (i) Methylidene equilibrium (**K$_1$**, forward and reverse rate constants) = varied (0.001 – 3), (ii) methylidene to alkylidene (**k$_2$** = 1), (iii) alkylidene to product (**k$_3$** = 10)

The catalytic cycle for the RCM of both **4.5** and **4.24** is fairly complex (as shown in Figure 4.3) and involves multiple reversible and irreversible steps that are difficult to observe experimentally. Only recently has it become possible to experimentally elucidate the potential energy surface (i.e., the relative energy of intermediates and transition states) for the productive component of RCM.[9]

Due to the limitations described above, we turned to kinetic modeling in order to reproduce the selectivity curves in Figure 4.6 and Figure 4.11 and to further our understanding of the reactions giving rise to degenerate metathesis. A simple kinetic model that accounts for catalyst initiation, initial formation of either an alkylidene or methylidene, degenerate exchange, and productive metathesis was developed using IBM's Chemical Kinetics Simulator.[12] Since we could not determine rate constants experimentally, arbitrary rate constants were chosen and varied relative to one another. We chose a Ru methylidene as the active species for degenerate metathesis since we assumed intramolecular cyclization ($\mathbf{k_3}$) from alkylidene **4.9** would be much faster than intermolecular reactions (e.g., degenerate metathesis). As shown in Figure 4.12, by progressively increasing the forward and reverse rate constants corresponding to degenerate exchange, we were able to reproduce the experimentally observed selectivity curves. Obviously, this assumes that all other rate constants remain constant across the entire catalyst series, which we later determined not to be true (Chapter 5). Nevertheless, this simple model effectively captures the experimentally observed behavior of catalysts **4.14**–**4.21**. Moreover, it also provides a framework that can be used when rate constants for productive and degenerate metathesis become available from theoretical and experimental studies.

Degenerate Metathesis and Ethenolysis

Ethenolysis is the reaction of an internal olefin with ethylene to generate thermodynamically disfavored terminal olefins (Figure 4.13). There is a significant interest in this reaction as a method for converting fatty acids derived

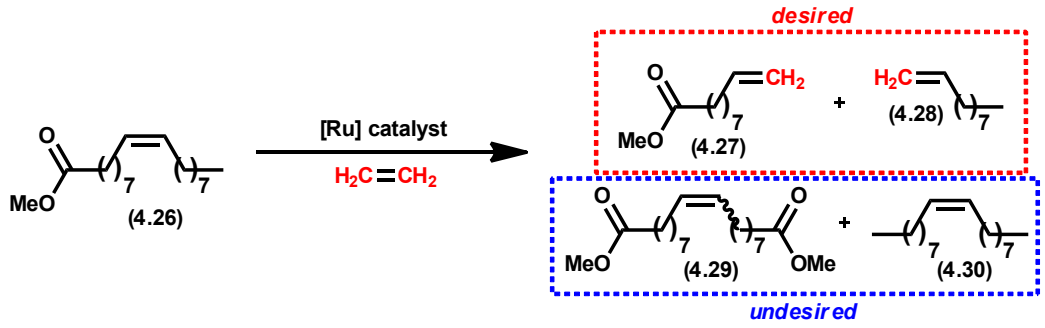

Figure 4.13. Ethenolysis of methyl oleate (**4.26**)

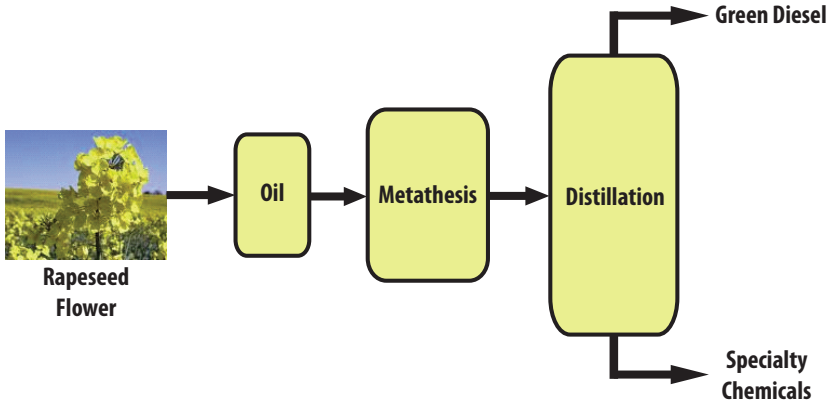

Figure 4.14. Incorporation of ethenolysis of seed oils into an industrial process for fuel and specialty chemical production

from renewable biomass into valuable commercial products (Figure 4.14).[13] Therefore, the development of a suitable catalyst to effect such a process would facilitate the green synthesis of commodity chemicals from renewable source materials instead of from petroleum. Unfortunately, because ethenolysis is thermodynamically disfavored relative to cross-metathesis (CM), selectivity, or the ratio of terminal olefins (desired) to internal olefins, is often low. In order to develop a commercially viable process, the selectivity and activity (TON) of current catalysts, based on both Ru and Mo, must be improved significantly.

During the course of our investigations into degenerate metathesis, we noted that catalysts with a higher selectivity for degenerate metathesis

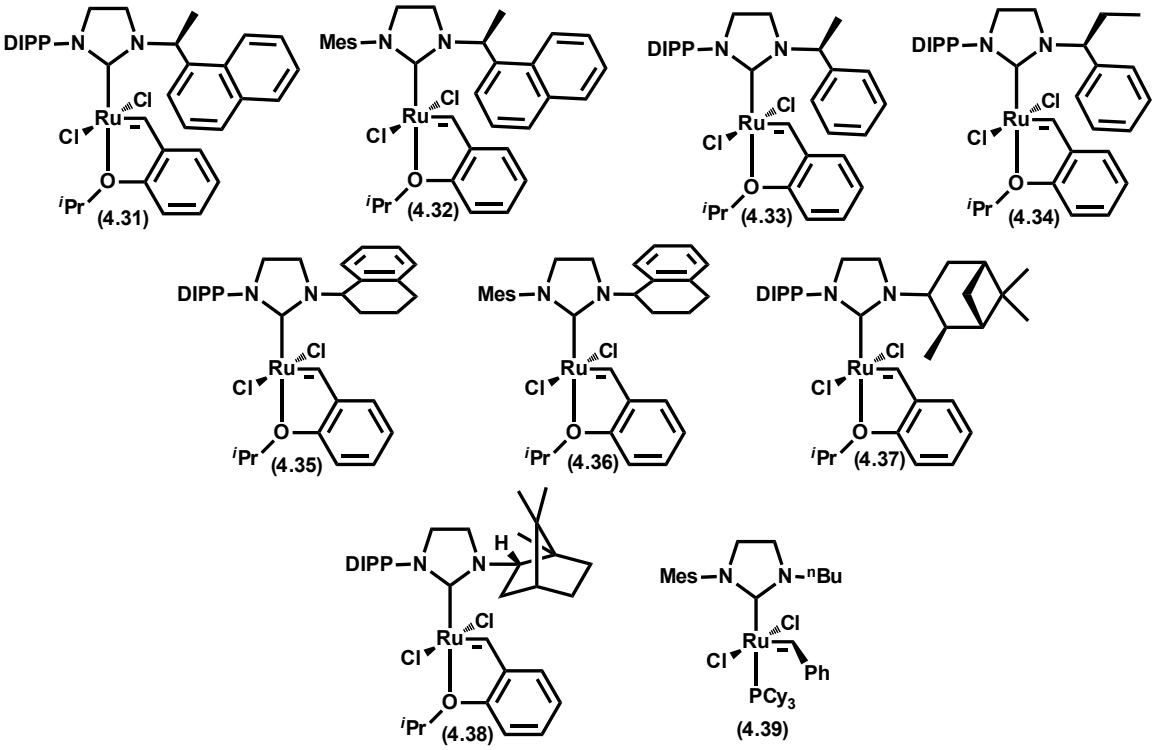

Figure 4.15. Catalysts examined for the ethenolysis of **4.26**

Tabel 4.1. Catalyst comparison for the ethenolysis of **4.26**

entry	catalyst	Conv., %[b]	Selectivity, %[c]	Yield, %[d]	TON[e]
1	**4.31**	54	86	46	4620
2	**4.32**	11	77	9	845
3	**4.33**	52	86	45	4450
4	**4.34**	42	86	36	3600
5	**4.35**	59	87	51	5070
6	**4.36**	17	69	11	1120
7	**4.37**	52	89	46	4604
8	**4.38**	15	95	15	1460
9	**4.39**	40	79	31	3080

[a] Reaction conditions were 100 ppm of catalyst in neat **4.26** with 150 psi ethylene for 6 h at 40 °C. [b] Conv. = 100 –[(final moles **4.26**) x 100/(initial moles **4.26**)]. [c] Selectivity = (moles **4.27** + **4.28**) x 100/(moles total product). [d] Yield = (moles **4.27** + **4.28**) x 100/(initial moles **4.26**). [e] TON = yield x [(moles of **4.26**)/moles of catalyst)]. Determined by gas chromotography (GC)

were also more effective ethenoylsis catalysts. For example, CAAC-based catalyst **4.20** underwent ca. one degenerate TON for every productive one and has been reported to be one of the most selective Ru-based ethenolysis catalysts.[10] Based on this result, we hypothesized that N-aryl/N-alkyl NHC-based catalysts such as **4.19** and **4.21** would also show good selectivity in ethenolysis reactions, without the need for a relatively exotic CAAC.

Unfortunately, when the ethenolysis of **4.26** was attempted with catalysts **4.19** and **4.21**, only catalyst decomposition was observed under our experimental conditions. This is not a surprising result considering neither catalyst reached very high TON in the RCM of **4.5** or **4.24**. Fortunately, several complexes with similar motifs, which were originally designed for asymmetric olefin metathesis, were found to catalyze the ethenolysis of **4.26**. As shown in Table 4.1, catalysts **4.31**–**4.39** exhibited selectivities for the desired products **4.27** and **4.28** of around 80% or above and demonstrated good TON. For comparison, under the same reaction conditions, catalyst **4.14** yielded a relatively low selectivity of 44% at a TON of 2800. On the other hand, a selectivity of 92% was measured for the ethenolysis of **4.26** catalyzed by **4.20**, which is comparable to the selectivities measured for catalysts **4.31**–**4.39**. Recall that **4.20**, as well as catalysts similar in structure to **4.31**–**4.39** displayed increased selectivity for degenerate metathesis. With this in mind, the above results clearly demonstrate that there is a correlation between degenerate selectivity and selectivity for terminal olefins (**4.27** and **4.28**) in ethenolysis. An understanding of this relationship is critical for the development of new ethenolysis catalysts for industrial applications.

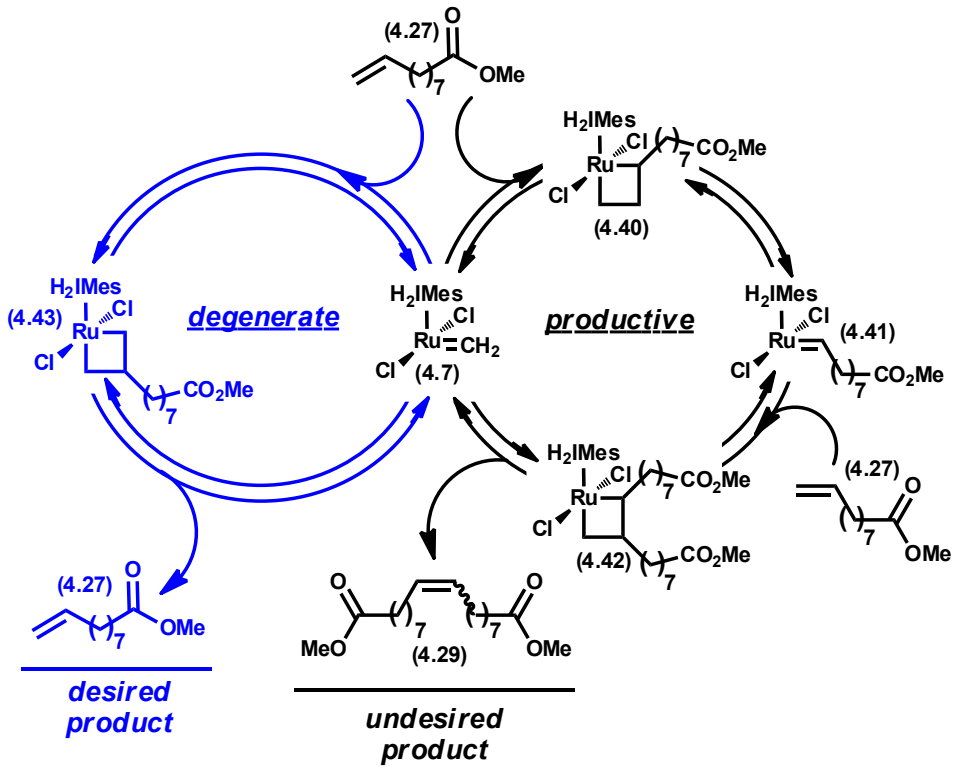

Figure 4.16. Degenerate (blue, left) and productive (black, right) metathesis pathways in the ethenolysis of **4.26**

Due to the high ethylene pressures used in ethenolysis, a propagating methylidene (**4.7**) is the most likely active species.[10] Starting from this intermediate, the catalyst has two choices which affect the selectivity observed in the ethenolysis reaction (Figure 4.16). If an α-substituted ruthenacycle (**4.40**) is formed, a productive metathesis cycle is initiated and undesired product is formed (**4.29**). In contrast, formation of a β-ruthenacycle (**4.43**) from **4.7** yields no change in the concentration of desired product **4.27**. [Note that degenerate metathesis may also proceed through an α,α'-ruthenacycle (e.g. **4.10**) such that formation of **4.40** does not necessarily lead to generation of **4.29** (not shown)]. Regardless of the identity of the degenerate propagating species, we have already established that certain catalysts are more susceptible to degenerate metathesis. As such, these same

catalysts prefer the degenerate pathway (blue) in Figure 4.16; thereby reducing the consumption of the desired products (**4.27** and **4.28**) after their formation. In other words, in the ethenolysis of **4.26**, selectivity for degenerate metathesis is actually beneficial!

Conclusions and Future Outlook

Using a SYMYX core robotic module, we were able to rapidly screen a wide variety of metathesis catalysts in an isotopic cross-over assay that effectively measured the amount of degenerate (nonproductive) to productive olefin metathesis. The structure of the catalyst, in particular the nature of the NHC, was found to have a substantial effect on a catalysts' selectivity for degenerate over productive metathesis. Specifically, N-aryl/N-aryl NHC-based catalysts displayed a preference for productive metathesis while N-aryl/N-*alkyl* catalysts demonstrated much lower preferences for productive metathesis. We also investigated the effects of temperature and substrate concentration on degenerate selectivity, but found these effects to be less significant compared to changes caused by catalyst structure.

We also investigated the consequences of degenerate metathesis selectivity in the ethenolysis of methyl oleate (**4.26**), a reaction with potential industrial applications. For this reaction, catalysts with structures known to increase susceptibility to degenerate metathesis were the most selective for the desired terminal olefin products of ethenolysis. In contrast, productive metathesis-selective catalysts exhibited poor selectivity for the desired ethenolysis products. These results demonstrate that in some circumstances, selectivity for degenerate metathesis can actually be beneficial. With this result in mind, future work should

focus on developing degenerate-selective catalysts that are capable of extremely high TON in ethenolysis reactions. Clearly, CAAC-based catalysts, such as **4.20**, appear to be promising in this regard.

Experimental

General Information: All reactions were carried out in dry glassware under an argon atmosphere using standard Schlenk techniques or in a Vacuum Atmospheres Glovebox under a nitrogen atmosphere unless otherwise specified. All solvents were purified by passage through solvent purification columns and further degassed with argon.[15] NMR solvents were dried over CaH_2 and vacuum transferred to a dry Schlenk flask and subsequently degassed with argon. Commercially available reagents were used as received unless otherwise noted. Silica gel used for the purification of organometallic compounds was obtained from TSI Scientific, Cambridge, MA (60 Å, pH 6.5-7.0).

Catalysts **4.14**, **4.15**, **4.16**, and **4.17** are commercially available and were used as received. **4.18**[16] and **4.20**[10] and **4.31**–**4.39**[17] were prepared according to the literature procedure. Productive TONs were measured using an Agilent 6850 Network GC equipped with a HP-1 column (L = 30 m, I.D. = 0.32 mm, Film = 0.25 μm). Response factors were calculated for all compounds prior to determining conversion. Degenerate TONs were measured with an Agilent 6200 Series TOF LC/MS equipped with an Agilent 1200 series HLPC stack using a 100% MeCN Direct Inject method.

Preparation of 4.19: **S1**[18] (91 mg, 0.41 mmol), methyl tosylate (92 mg, 0.49

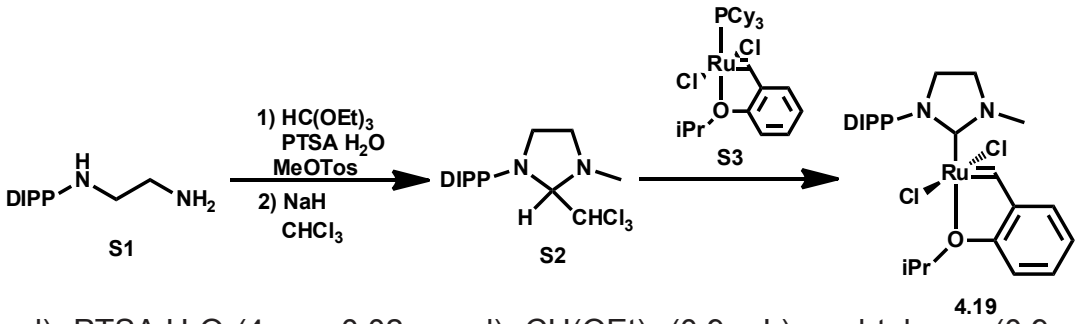

mmol), PTSA·H_2O (4 mg, 0.02 mmol), $CH(OEt)_3$ (0.9 mL), and toluene (0.9 mL) were placed in a 20 mL scintillation vial and sealed under air using a teflon cap. The sealed vial was heated to 110 °C for 14 h and then allowed to cool to RT. Et_2O was added to precipitate the product and the solution was stirred for 2 h after which the solvent was decanted off and the remaining solid dried under vacuum. The crude product (280 mg, 0.67 mmol) was dissolved in dry $CHCl_3$ (10 mL) in a Schlenk flash and 95% NaH (97 mg, 4.0 mmol) was added in portions. The flask was sealed and heated to 55 °C for 14 h. After cooling, the solution was diluted with Et_2O and passed through a pad of silica gel. The filtrate was concentrated without heating and used without further purification. A 50 mL round-bottom flask was dried and charged with **S2** (112 mg, 0.34 mmol), **S3** (103 mg, 0.17 mmol), and THF (20 mL). The flask was heated to 70 °C under argon for 10 h and then concentrated. The residue was dissolved in a minimal amount of C_6H_6 and purified by flash chromatography on silica gel eluting with 10% Et_2O/Pentane to collect a brown band (**S3**), and then 30% Et_2O/Pentane to collect a green/tan band (**7**, 7 mg, 7%). ^{1}H NMR (500 MHz, C_6D_6): δ 1.04 (m, 6H), 1.11 (m, 6H), 1.72 (m, 6H), 2.92 (m, 2H), 3.34 (m, 4H), 3.82 (s, 3H), 4.63 (sept, *J* = 3.5 Hz, 1H), 6.42 (dd, *J* = 8.5 Hz, *J* = 3.5 Hz, 1H), 6.67 (dt, *J* = 7.5 Hz, 4 Hz, 1H), 7.08 (m, 2H), 7.19 (dd, *J* = 7.5 Hz, *J* = 4 Hz, 2H), 7.36 (dt, *J* = 8 Hz, 4 Hz, 1H), 16.33 (s, 1H). ^{13}C NMR (126 MHz, C_6D_6) δ

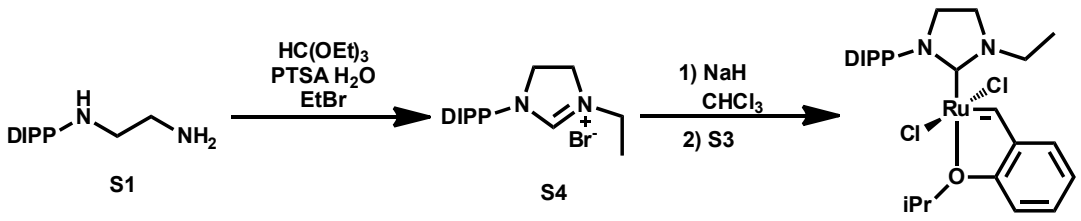

270.08, 211.51, 153.58, 149.32, 148.20, 144.18, 138.64, 130.10, 129.19, 128.66, 125.44, 122.81, 122.37, 113.49, 107.56, 75.51, 55.44, 51.29, 38.79, 30.54, 28.49, 26.03, 24.57, 22.52. HRMS (FAB+): Calculated: 564.1249, Found: 562.1240.

Preparation of 4.21: **S1** (202 mg, 0.917 mmol), EtBr (82 µL, 1.1 mmol), PTSA·H_2O (9 mg, 0.05 mmol), $CH(OEt)_3$ (2.25 mL), and toluene (2.25 mL) were placed in a 20 mL scintillation vial and sealed under air using a Teflon cap. The vial was heated to 110 °C for 16 h, after which it was cooled to RT and the toluene was removed in vacuo. Et_2O (ca. 8 mL) was added to the resulting solution and it was stirred vigorously for 1 h. The Et_2O was decanted off and the remaining precipitate was washed with copious amounts of Et_2O and dried under vacuum. Flash chromatography on silica gel using 7% MeOH:CH_2Cl_2 gave **S4** (92 mg, 30%) as an off white solid. ^{1}H NMR (300 MHz, $CDCl_3$): δ 9.50 (s, 1H), 7.34–7.27 (m, 1H), 7.11 (d, *J* = 7.8 Hz, 2H), 4.33–4.24 (m, 2H), 4.17–4.07 (m, 2H), 3.94 (q, *J* = 7.2 Hz, 2H), 2.78 (dt, *J* = 13.6, 6.8 Hz, 2H), 1.32–1.24 (m, 4H), 1.15 (dd, *J* = 6.8, 3.8 Hz, 12H).

S4 (64 mg, 0.189 mmol) was placed in a 20 mL vial followed by dry $CHCl_3$ (2 mL). 95% NaH (23 mg, 0.945 mmol) was added in small portions after which the vial was sealed under nitrogen and heated to 55 °C for 10 h. After cooling to RT, the solution was diluted with Et_2O, filtered through a small pad of silica washing with Et_2O, and conc. without heating to give the chloroform adduct (48 mg, 67%) which

was used without further purification. A 100 mL RB flask was dried and charged with the chloroform adduct (306 mg, 0.81 mmol), **S3** (361 mg, 0.60 mmol), and THF (50 mL). The RB was heated to 70 °C for 24 h after which it was cooled to RT and conc. in vacuo. The resulting residue was dissolved in a minimal amount of PhH and flashed on silica gel using 30% Et_2O/Pentane to collect the left over **S3** followed by 60% Et_2O/Pentane to collect **4.21** (40 mg, 9%). ^1H NMR (500 Mhz, C_6D_6): δ 1.01 (d, 6H, *J* = 6.6 Hz), 1.09 (d, 6H, *J* = 6.6 Hz), 1.28 (t, 3H, *J* = 6.6 Hz), 3.05 (m, 2H), 3.30 (sept, 2H, 6.6 Hz), 3.42 (m, 2H), 4.50 (d, 2H, *J* = 6.6 Hz), 4.59 (sept, 1H, *J* = 6 Hz), 6.38 (d, 1H, *J* = 8.4 Hz), 6.65 (dt, 1H, *J* = 7.2 Hz, *J* = 1.2 Hz), 7.04-7.08 (m, 2H), 7.11 (br s, 3H), 7.16 (s, 1H), 7.17 (s, 1H), 7.33 (t, 1H, *J* = 7.8 Hz), 16.32 (s, 1H). ^{13}C NMR (151 MHz, C_6D_6) δ 285.32, 210.77, 153.55, 150.67, 149.36, 144.29, 138.68, 130.08, 129.21, 128.90, 128.66, 125.44, 122.82, 122.46, 113.51, 75.41, 55.37, 47.67, 47.25, 28.53, 26.04, 24.59, 22.52, 14.19. HRMS (FAB+): Calculated: 578.1405, Found: 578.1433.

Preparation of 4.5-d_2: Propargyl alcohol (**4.1**, 4 mL, 67.7 mmol), K_2CO_3 (2.8 g, 20.3 mmol), and D_2O (12 mL, Aldrich 99.9%) were combined in a Biotage 20 mL microwave vial with a stir bar. Two other vials with the same reagents were prepared and all three were microwaved at 100 °C for 10 min using a Biotage Initiator microwave. The three vials were combined in a separatory funnel and NaCl was added. The aqueous layer was extracted with Et_2O (3X) and the organic layers were combined, dried with Na_2SO_4, and carefully conc. to yield deuterated propargyl alcohol showing ca. 90% D incorporation. The same procedure was repeated to obtain deuterated propargyl alcohol (**4.2**, 7.06 g, 60%) with >96%

incorporation after distillation under Ar. ^{1}H NMR ($CDCl_3$, 300 MHz): δ 4.23 (s, 2H).

A 250 mL round-bottomed flask was dried and charged with $LiAlH_4$ (4.94 g, 130 mmol), and Et_2O (150 mL) in a glovebox. The flask was capped with an addition funnel, removed from the box and cooled to 0 °C under Ar. Propargyl alcohol-d_2 (**4.2**, 7.06 mL, 121.6 mmol) was dissolved in Et_2O (28 mL) and added to the addition funnel. The alcohol solution was added drop-wise to the LAH suspension at 0 °C over a period of 1 h after which the solution was allowed to warm to RT and stirred for 6 h. D_2O (5 mL) was added slowly at 0 °C followed by a 15 wt% NaOH in D_2O solution (5 mL). Finally, D_2O (15 mL) was added quickly and the suspension was allowed to stir at RT overnight. $MgSO_4$ and celite were added and the suspension was filtered through celite, washing with Et_2O, and the filtrate was conc. Allyl alcohol-d_3 (4 g, 55%) was recovered via fractional distillation under Ar. ^{1}H NMR ($CDCl_3$, 300 MHz): δ 5.98 (m, 1H), 4.14 (t, J = 6 Hz, 2H). A 250 mL RB flask was dried and charged with dry triethylamine (6.4 mL, 44.9 mmol), allyl alcohol-d_3 (2.5 g, 40.8 mmol), and Et_2O (120 mL) and cooled to 0 °C. MsCl (3.5 mL, 44.9 mmol) was added drop-wise and the reaction was stirred at 0 °C for 1 h after which it was warmed to RT and stirred for 12 h. The reaction was quenched with H_2O, and the aqueous layer was extracted with Et_2O (3X). The organic layers were combined and stirred with sat. $NaHCO_3$ for 30 minutes after which the org. layer was separated, washed with brine, and dried with $MgSO_4$, and conc. to yield mesylate-d_2 (**4.3**, 1.5 g, 26%) which was used immediately without further purification.

A 100 mL round-bottomed flask was dried and charged with 60% NaH (0.48 g, 20.1 mmol) and THF (20 mL). Diethyl allyl malonate (**4.4**, 3.2 mL, 15.9 mmol)

was added drop-wise and the solution was heated to 60 °C for 30 min. After cooling to RT, mesylate-d_2 (**4.3**, 0.96 g, 6.9 mmol) was added slowly as solution in THF and the reaction was heated to 60 °C for 12 h. After cooling to RT, the reaction was quenched with sat. NH_4Cl and the aq. layer was extracted with Et_2O (2X). The organic layers were combined, dried over Na_2SO_4 and conc. to give the crude product which was purified via flash chromatography on silica gel (5% EtOAc/

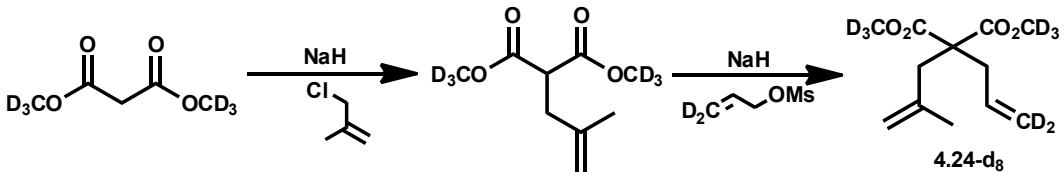

Hexanes) to give **4.5-d$_2$** (1.87 g, 81%). ^{1}H NMR (300 MHz, $CDCl_3$) δ 5.65 (dddd, *J* = 14.8, 10.7, 9.3, 7.4 Hz, 1H), 5.14–5.07 (m, 1H), 4.22–4.13 (m, 2H), 2.63 (dd, *J* = 7.4, 1.3 Hz, 2H), 1.27–1.22 (m, 3H). ^{13}C NMR (151 MHz, $CDCl_3$) δ 170.65, 132.27, 132.04, 119.02, 61.12, 57.17, 36.67, 36.57, 14.04.

HRMS (FAB+): Calculated: 243.1570, Found: 243.1560.

Preparation of 24-d$_8$: A 100 mL round-bottomed flask was dried and charged with 60% NaH (0.92 g, 38 mmol) and THF (30 mL). Dimethyl malonate-d_6[19] (2.5 mL, 20.9 mmol) was added drop-wise and the reaction was heated to 60 °C for 30 min. After cooling to RT, 1-chloro-2-methyl propene (2.27 mL, 23 mmol) was added drop-wise and the reaction was again heated to 60 °C for 12 h. After cooling to RT, the reaction was quenched with sat. NH_4Cl and extracted with Et_2O (3X). The organic layers were combined, dried over Na_2SO_4 and conc. to give the crude product which was purified via flash chromatography (7% EtOAc/

Hexanes) on silica gel (2.23 g, 77%). ^{1}H NMR (300 MHz, $CDCl_3$) δ 4.78 (s, 3H), 4.71 (s, 4H), 3.61 (td, *J* = 7.8, 1.9 Hz, 2H), 2.61 (d, *J* = 7.1 Hz, 7H), 1.73 (s, 10H).

The same alkylation procedure as above with the previous product (1.9 g, 9.8 mmol), mesylate-d_2 (**4.3**, 1.5 g, 10.8 mmol), and 60% NaH (0.43 g, 17.9 mmol) yielded **4.24-d$_8$** (1.62 g, 73%). ^{1}H NMR (300 MHz, $CDCl_3$) δ 5.66 (s, 1H), 4.86 (s, 1H), 4.72 (s, 1H), 2.70 (s, 1H), 2.66 (d, *J* = 7.4 Hz, 1H), 1.52 (s, 1H). ^{13}C NMR (151 MHz, $CDCl_3$) δ 171.43, 140.33, 132.35, 117.47, 115.67, 57.23, 40.23, 36.80, 23.02. HRMS (FAB+): Calculated: 235.1780, Found: 235.1796.

Typical Reaction Procedure: The RCM of **4.5-d$_2$** and **4.24-d$_8$/4.24-d$_0$** using the catalysts described were conducted using a Symyx™ Technologies Core Module (Santa Clara, CA) housed in an mBraun nitrogen-filled glovebox and equipped with Julabo LH45 and LH85 temperature-control units for separate positions of the robot tabletop.

For experiments where aliquots were taken during the course of the reaction, the entire operation could be performed on 12 reactions simultaneously in 1 or 2 mL vials by an Epoch software-based protocol as follows. To prepare catalyst stock solutions (1 mM), 20 mL glass scintillation vials were charged with catalyst (5 μmole) and diluted to 5 mL total volume in toluene. Catalyst solutions, 6 to 800 μL depending on desired final catalyst loading, were transferred to reaction vials and solvent was removed via centrifugal evaporation. The catalysts were preheated to 50 °C using the LH45 unit, and stirring was started. Substrates (0.1 mmol), containing dodecane (0.025 mmol) as an internal standard, were dispensed simultaneously to 4 reactions at a time using one arm of the robot

equipped with a 4-needle assembly. Immediately following substrate addition, toluene was added to reach the desired reaction molarity. The reaction vials were left open to the glovebox atmosphere during the course of the reaction.

After the 2 minutes required for completion of the transfer, 50 μL aliquots of each reaction were withdrawn using the other robot arm and dispensed to 1.2 mL septa-covered vials containing 5% v/v ethyl vinyl ether in toluene cooled to −20 °C in two 96-well plates. The needle was flushed and washed between dispenses to prevent transfer of the quenching solution into the reaction vials. 16 time points were sampled at preprogrammed intervals and the exact times were recorded by the Epoch protocol. All reactions were conducted in either duplicate or triplicate in order to ensure reproducibility.

Alternatively, reactions could also be performed on the bench as follows. In a glove box, 126 μL of a stock solution prepared from **4.5-d$_2$** (244 μL, 1 mmol), dodecane (23 μL, 0.1 mmol), and toluene (1 mL) was added to 2 (duplicate) or 3 (triplicate) 4 mL scintillation vials equipped with stir bars. Toluene (0.9 mL) was added and the vials were sealed with septa caps, removed from the box, and heated to 50 °C under a continuous flow of Ar. The desired amount of catalyst (depending on the loading) was injected as a solution in toluene after which 50 μL aliquots were removed over time and injected into chilled GC vials containing toluene and ca. 5% v/v ethyl vinyl ether. Reactions conducted on the bench showed identical behavior to those conducted using the Symyx™ robot. The best results were obtained from the following catalyst loadings:

4.15—1000 ppm, **4.14, 4.16, 4.17, 4.18**—250 ppm, **4.20**—500 ppm, **4.18**—5000

ppm, **21**—1000 ppm.

Productive TON Determination: Samples for GC analysis were obtained by adding a 50 µL reaction aliquot to 1 mL of toluene containing ca. 5% v/v ethyl vinyl ether at either -10 °C (bench) or -30 °C (robot). GC response factors were determined for all starting materials and products. Dodecane was used as an internal standard. To determine conversion factors, stock solutions of each compound were prepared and used to make various solutions at different [substrate]/[dodecane] ratios. The ratio of the area percent data was plotted against the molar ratio of each solution and the corresponding factor was determined by fitting the data to a linear trendline Instrument conditions: Inlet temperature: 85 °C; Detector temperature: 250 °C; hydrogen flow: 30 mL/min' air flow: 400 mL/min; constant col + makeup flow: 25 mL/min. GC Method: 85 °C for 1.5 min, followed by temperature increase of 15 °C/min to 160 °C, followed by a second temperature increase of 80 °C/min to 210 °C with a subsequent isothermal period at 210 °C for 5 min. Total run time was 13.1 min including a 210 °C post-run for 1 min. GC data for each timepoint were analyzed according to the following model spreadsheet.

Aliquot	dodecane	P	SM	ratio P	ratio SM	P (mmol)	SM (mmol)	conv.
1	**A**	**B**	**C**	**B/A**	**C/A**	0.01[1.37(**B/A**)]	0.01[1.14(**C/A**)]	P (mmol)/[P (mmol) + SM (mmol)]

Table S1. Example for calculation of **4.5-d$_2$** conversions.

Degenerate TON Determination: Aliquots taken as above were injected (0.75 µL) into an Agilent 6200 Series TOF LC/MS instrument using a direct-inject 100% MeCN

method. Relative isotopologue counts were obtained from the positive ion spectra and showed good reproducibility when the same sample was injected multiple times.

Using the LCMS-TOF, the counts of **4.5-d_0** and **4.5-d_4** were determined and used to compute a conversion after subtracting the corresponding values for the stock solution (to account for any isotopologues already present). Conversions that resulted in negative values were thrown out. The conversions to **4.5-d_0** and **4.5-d_4** were then each multiplied by 2 and summed together to obtain the total degenerate conversion. This factor of 2 helps account for the degenerate processes that generate the same isotopologue (e.g., **4.5-d_0** reacting with Ru=CH_2 to form **4.5-*d_0***). Finally, the degenerate TONs were calculated based on the catalyst loading and compared to the productive TONs which were calculated as above.

Kinetic Modeling: The following model was used in IBM's Chemical Kinetics Simulator. Rate of initial methylidene formation = 1; Rate of initial alkylidene formation = 1; Methylidene equilibrium (forward and reverse rates) = varied; Rate of methylidene to alkylidene = 1; Rate of alkylidene to product = 10.

Procedure for Ethenolysis of Methyl Oleate (4.25): Ethenolysis reactions were carried out using research-grade methyl oleate (> 99%) that was purified by storage over actived alumina followed by filtration. The experiments were set up in a glove box under an atmosphere of argon. Methyl oleate was charged in a Fisher-Porter bottle equipped with a stir bar. A solution of ruthenium catalyst of an appropriate concentration was prepared in dry dichloromethane, and the desired volume of this solution was added to the methyl oleate. The head of the Fisher-Porter bottle was equipped with a pressure gauge and a dip-tube was

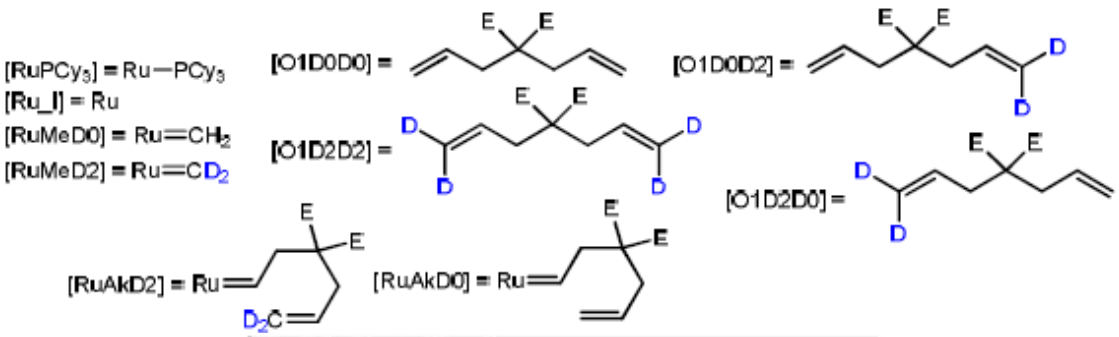

[RuPCy3] => [Ru_I]
[Ru_I] + [O1d0d2] => [RuMeD0]
[Ru_I] + [O1d2d0] => [RuMeD2]
[RuMeD0] + [O1d2d0] <=> [O1d0d0] + [RuMeD2]
[RuMeD2] + [O1d0d2] <=> [O1d2d2] + [RuMeD0]
[RuMeD0] + [O1d0d2] <=> [RuMeD0] + [O1d0d2]
[RuMeD2] + [O1d2d0] <=> [RuMeD2] + [O1d2d0]
[RuMeD0] + [O1d2d0] => [RuAkd0] + [CH2CD2]
[RuMeD2] + [O1d0d2] => [RuAkd2] + [CH2CD2]
[RuMeD0] + [O1d0d2] => [RuAkd2] + [CH2CH2]
[RuMeD2] + [O1d2d0] => [RuAkd0] + [CD2CD2]
[RuAkd0] => [P] + [RuMeD0]
[RuAkd2] => [P] + [RuMeD2]
[RuMeD0] + [O1d2d2] => [RuAkd2] + [CH2CD2]
[RuMeD0] + [O1d0d0] => [RuAkd0] + [CH2CH2]
[RuMeD2] + [O1d2d2] => [RuAkd2] + [CD2CD2]
[RuMeD2] + [O1d0d0] => [RuAkd0] + [CH2CD2]
[Ru_I] + [O1d0d2] => [RuAkd2]
[Ru_I] + [O1d2d0] => [RuAkd0]

adapted on the bottle. The system was sealed and taken out of the glove box to the ethylene line. The vessel was then purged with ethylene (polymer purity 99.9% from Matheson Tri Gas) for 5 minutes, pressurized to 150 psi, and placed in an oil bath at 40°C. The reaction was monitored by collecting samples via the dip-tube at different reaction times. Prior to GC analysis, the reaction aliquots were quenched by adding a 1.0 M isopropanol solution of tris-hydroxymethylphopshine (THMP) to each vial over the course of 2–3 hours. The samples were then heated for over an 1 hour at 60°C, diluted with distilled water, extracted with hexanes and analyzed by gas chromatography (GC). The GC analyses were run using a flame ionization detector. Column: Rtx-5 from Restek (30 m x 0.25 mm (i.d.) x 0.25 μm

film thickness. GC and column conditions: injection temperature, 250 °C; detector temperature, 280 °C; oven temperature, starting temperature, 100 °C; hold time, 1 min. The ramp rate was 10 °C/min to 250 °C, and the temperature was then held at 250 °C for 12 min. Carrier gas: Helium

References

(1) (a) Casey, C. P.; Tuinstra, H. E. *J. Am. Chem. Soc.* **1978**, *100*, 2270. (b) Casey, C. P.; Tuinstra, H. E.; Saeman, M. C. *J. Am. Chem. Soc.* **1976**, *98*, 608. (c) Handzlik, J. *J. Mol. Cat. A* **2004**, *218*, 91. (d) McGinnis, J.; Katz, T. J.; Hurwitz, S. *J. Am. Chem. Soc.* **1976**, *98*, 605. (e) Tanaka, K.; Takeo, H.; Matsumura, C. *J. Am. Chem. Soc.* **1987**, *109*, 2422.

(2) Janse van Rensburg, W.; Steynberg, P. J.; Meyer, W. H.; Kirk, M. M.; Forman, G. S. *J. Am. Chem. Soc.* **2004**, *126*, 14332.

(3) Meek, S.M.; Malcolmson, S.J.; Li, B.; Schrock, R. R.; Hoveyda, A.H. *J. Am. Chem. Soc.* **2009**, *131*, 16407.

(4) (a) Ritter, T.; Hejl, A.; Wenzel, A. G.; Funk, T. W.; Grubbs, R. H. *Organometallics* **2006**, *25*, 5740. (b) Kuhn, K. M.; Bourg, J.-B.; Chung, C. K.; Virgil, S. C.; Grubbs, R. H. *J. Am. Chem. Soc.*, **2009**, *131*, 5313.

(5) Ritter, T.; Hejl, A.; Wenzel, A. G.; Funk, T. W.; Grubbs, R. H. *Organometallics* **2006**, *25*, 5740.

(6) http://accelrys.com/. Accessed 06-11-2012

(7) Stewart, I. C.; Keitz, B. K.; Kuhn, K. M.; Thomas, R. M.; Grubbs, R. H. *J. Am. Chem. Soc.* **2010**, *132*, 8534.

(8) (a) Sanford, M. S.; Love, J. A.; Grubbs, R. H. *J. Am. Chem. Soc.* **2001**, *123*,

6543. (b) Sanford, M. S. Thesis, California Institute of Technology, 2001.

(9) (a) Samojłowicz, C.; Bieniek, M.; Grela, K. *Chem. Rev.* **2009**, *109*, 3708. (b) Vougioukalakis, G. C.; Grubbs, R. H. *Chem. Rev.* **2010**, *110*, 1746.

(10) (a) Romero, P. E.; Piers, W. E.; McDonald, R. *Angew. Chem. Int. Ed.* **2004**, *43*, 6161. (b) Rowley, C. N.; van der Eide, E. F.; Piers, W. E.; Woo, T. K. *Organometallics* **2008**, *27*, 6043. (c) van der Eide, E. F.; Romero, P. E.; Piers, W. E. *J. Am. Chem. Soc.* **2008**, *130*, 4485. (d) Leitao, E. M.; van der Eide, E. F.; Romero, P. E.; Piers, W. E.; McDonald, R. *J. Am. Chem. Soc.* **2010**, *132*, 2784. van der Eide, E. F.; Piers, W. E. *Nature Chemistry*. **2010**, *2*, 571.

(11) (a) Anderson, D. R.; Lavallo, V.; O'Leary, D. J.; Bertrand, G.; Grubbs, R. H. *Angew. Chem. Int. Ed.* **2007**, *46*, 7262. (b) Anderson, D. R.; Ung, T. A.; Mkrtumyan, G.; Bertrand, G.; Grubbs, R. H.; Schrodi, Y. *Organometallics* **2008**, *27*, 563.

(12) *Chemical Kinetics Simulator*, version 1.01; International Business Machines: Almaden Research Center, 1996.

(13) (a) Burdett, K. A.; Harris, L. D.; Margl, P.; Maughon, B. R.; Mokhtar-Zadeh, T.; Saucier, P. C.; Wasserman, E. P. *Organometallics* **2004**, *23*, 2027. (b) Schrodi, Y.; Ung, T.; Vargas, A.; Mkrtumyan, G.; Lee, C. W.; Champagne, T. M.; Pederson, R. L.; Hong, S. H. *Clean* **2008**, *36*, 669.(c) Chikkali, S.; Mecking, S. *Angew. Chem. Int. Ed.* **2012**, *51*, 5802.

(14) Mandelli, D.; Jannini, M. J. D. M.; Buffon, R.; Schuchardt, U. *J. Am. Oil Chem. Soc.* **1996**, *73*, 229.

(15) Love, J.A.; Morgan, J.P.; Trnka, T.M.; Grubbs, R.H., *Angew. Chem. Int. Ed.* **2002**, *41*, 4035.

(16) Blum, A. P.; Ritter, T.; Grubbs, R. H. *Organometallics* **2007**, *26*, 2122.

(17) Thomas, R. M.; Keitz, B. K.; Champagne, T. M.; Grubbs, R. H. *J. Am. Chem. Soc.* **2011**, *133*, 7490.

(18) Marshall, C.; Ward, M. F.; Skakle, J. M. S. *Synthesis* **2006**, 1040.

(19) Kolsaker, P.; Kvarsnes, A.; Storesund, H. *Org. Mass. Spec.* **1986**, *21*, 535.